

# Scattered Isergonic Profiles

JAMES J. ZIMMERMAN

**Abstract** □ Equations were developed for the geometric analysis of scatter in isergonic profiles as a function of vertical ( $\Delta\Delta H$ ), horizontal ( $\Delta\Delta S$ ), and perpendicular ( $d$ ) distances from the error line. Sigma ( $\sigma^-$ ) correlates with each of these quantities of the test series to produce statistics ( $F$  and  $r$ ) identical to those for correlation with  $\Delta G$ . The vertical distances,  $\Delta\Delta H$ , are shown to be identical to the substituent effect,  $\delta\Delta G$ ; thus, it is concluded that the Hepler approach of implicating a solvation mechanism on the basis of  $\rho$ - $\sigma$  correlations for these distances is not warranted. The uncertainty of points on the isergonic profile for the test series was determined using the joint confidence region ("error contour") approach. Statistical limits of the contour lengths overlapped extremely between members of the test series. To eliminate such overlap for series showing small ranges in substituent effects, extremely precise rate data would be required with  $N$  (number of data points) = 4 or 5 for the Arrhenius fits. A comparison between  $d$  values and the perpendicular half-widths ( $w/2$ ) of the error contours resulted in  $d > w/2$  for each member of the test series (excluding  $H$ ), proving that scatter in the profile could not result from experimental error. A further comparison between differences in  $d$ ,  $\Delta d$ , from suggested  $\beta$  lines for solvation and  $w/2$  values showed that a  $\beta$  range as large as  $45^\circ$  could be included in the error contour widths of the test series. Since the average reaction temperature,  $\bar{T}$ , fell within this range, solvation effects could not be distinguished statistically from error effects.

**Keyphrases** □ Solvation isergonic profiles—geometric analysis of scatter as a function of vertical, horizontal, and perpendicular distances from error line □ Isergonic profiles, solvation—geometric analysis of scatter as a function of vertical, horizontal, and perpendicular distances from error line □ Reaction mechanisms—solvation isergonic profiles, geometric analysis of scatter as a function of vertical, horizontal, and perpendicular distances from error line

Attempts to demonstrate the usefulness of entropy-enthalpy ( $\Delta H$  versus  $\Delta S$ ) profiles in augmenting the mechanistic descriptions of chemical reactions have been well documented (1). Recent publications attempted to extend them to enzyme reactions (2) and protein-small molecule interactions in general (3).

In many cases,  $\Delta H$  versus  $\Delta S$  profiles are linear; the slope of such profiles for either rate or equilibrium data yields  $\beta_i$ <sup>1</sup>, the isergonic<sup>2</sup> temperature (1, 2), in accordance with:

$$\delta\Delta H = \beta_i \delta\Delta S \quad (\text{Eq. 1})$$

where  $\delta$  = the Leffler-Grunwald operator for substituent or medium effects. The linearity of such profiles tends to confirm a common reaction mechanism for the members of a congeneric series, and the numerical value of  $\beta_i$  is potentially associated with a known reaction mechanism. Thus, a value of  $\beta_i \simeq 280^\circ\text{K}$  is customarily associated with an aqueous solvation mechanism for a series (4).

Hepler (5) showed that Eq. 1 is one relationship obtained from an exact thermodynamic analysis of the Hammett equation (Eq. 2) when  $\Delta H$  and  $\Delta S$  are temperature independent:

$$\log(k_x/k_H) = \rho\sigma \quad (\text{Eq. 2})$$

where  $\rho$  = reaction constant,  $\sigma$  = substituent constant, and

<sup>1</sup> The slope =  $R\beta_i$ ; when Arrhenius parameters  $E_a$  and  $\ln A$  are used for rate data.

<sup>2</sup> The general term isergonic is used here to include both isokinetic and isoequilibrium phenomena (Ref. 2).

$x$  and  $H$  refer to substituted and parent derivatives, respectively. As a result, congeneric series that obey Eq. 2 should also obey Eq. 1. However, some reaction series follow the Hammett relationship but their  $\Delta H$  versus  $\Delta S$  profiles are nonlinear or scattered (1). A rational explanation for the behavior of such series was discussed previously in terms of multiple interaction mechanisms and related compensation phenomena (1, 5).

## THEORETICAL

**Leffler-Grunwald Analysis of Scattered Isergonic Profiles**—According to Leffler and Grunwald (1), the scatter in  $\Delta H$  versus  $\Delta S$  profiles may be explained in terms of multiple contributions to the observed enthalpies and entropies. For a model based on a two-interaction mechanism, the enthalpy and entropy expressions are given by:

$$\delta\Delta H = \delta\Delta H' + \delta\Delta H'' \quad (\text{Eq. 3})$$

$$\delta\Delta S = \delta\Delta S' + \delta\Delta S'' \quad (\text{Eq. 4})$$

where the superscripts, ' and '', refer to two different but additive types of substituent contributions (e.g., resonance, inductive, steric, or solvation effects). These two contributions to the observed enthalpy and entropy would vary independently of one another for any given reaction series. Therefore, a plot of  $\Delta H$  versus  $\Delta S$  would not be expected to be linear. For the same reason, a plot of the Hammett equation (Eq. 2) would not be expected to be linear under these conditions.

On the other hand, when each of the two mechanisms is isergonically related (i.e.,  $\delta\Delta H' = \beta' \delta\Delta S'$  and  $\delta\Delta H'' = \beta'' \delta\Delta S''$ ):

$$\delta\Delta H = \beta' \delta\Delta S' + \beta'' \delta\Delta S'' \quad (\text{Eq. 5})$$

$$\delta\Delta S = \delta\Delta H'/\beta' + \delta\Delta H''/\beta'' \quad (\text{Eq. 6})$$

$$\delta\Delta G = [\beta' - T]\delta\Delta S' + [\beta'' - T]\delta\Delta S'' = [1 - (T/\beta')]\delta\Delta H' + [1 - (T/\beta'')]\delta\Delta H'' \quad (\text{Eq. 7})$$

From Eq. 7 it is apparent that for reactions run at  $T = \beta'$  or  $T = \beta''$ , the free energy expression will be simpler by one interaction mechanism. The same, however, is not true for the observed enthalpy and entropy expressions (Eqs. 5 and 6), which remain complex independent of  $T$  when  $\beta' \neq \beta''$  or  $\beta' \gg \beta''$ . In practice, then, it is possible to obtain linear Hammett plots even when the  $\Delta H$  versus  $\Delta S$  profile is scattered, provided that the reaction temperature is close to  $\beta'$  or  $\beta''$ .

**Hepler Analysis of Scattered Isergonic Profiles**—Hepler (4, 5) proposed a two-interaction model, which simplifies Eqs. 3 and 4 and permits the linearization of a scattered  $\Delta H$  versus  $\Delta S$  plot. According to the Hepler scheme, the prime and double-prime superscripts of Eqs. 3 and 4 refer to internal and external contributions of substituents, respectively. The internal contributions represent substituent interactions with the reaction center, and the environmental contributions represent substituent interactions with the solvent. By assuming an isergonic relationship for the environmental contributions and a negligible contribution from the internal entropy, Eq. 8 may be derived from Eqs. 3 and 4:

$$\delta\Delta H = \delta\Delta H' + \beta'' \delta\Delta S \quad (\text{Eq. 8})$$

where  $\beta''$  is the isergonic temperature for the solvation effect. The  $\delta\Delta H'$  quantity, corresponding to the internal enthalpy contribution, may now be calculated from Eq. 8 using the experimentally observed values of  $\delta\Delta H$  and  $\delta\Delta S$  and letting  $\beta'' = \bar{T}$ , the average temperature for the determinations<sup>3</sup> (5, 6). The free energy expression for the Hepler scheme is given by:

$$\delta\Delta G = \delta\Delta H' + (\beta'' - T)\delta\Delta S \quad (\text{Eq. 9})$$

<sup>3</sup> The reviewer of this manuscript appropriately commented that the Hepler scheme with  $270^\circ < \beta < 320^\circ$  is specifically applicable to water and similar solvents. In other solvent systems,  $\beta''$  for solvation may not necessarily approximate  $\bar{T}$ .

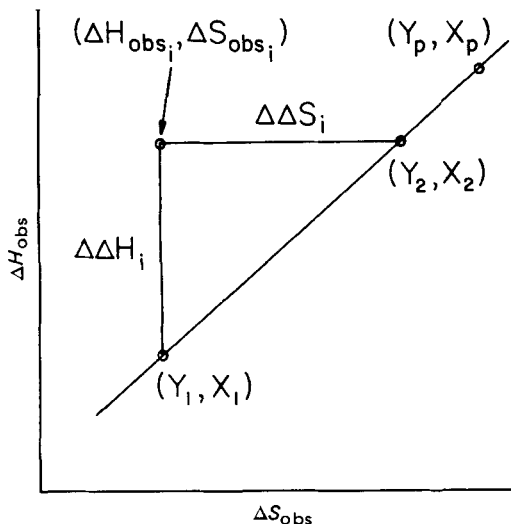


**Figure 1**—Diagram showing the vertical ( $\Delta\Delta H_i$ ) and horizontal ( $\Delta\Delta S_i$ ) distances of point  $(\Delta H_{obs_i}, \Delta S_{obs_i})$  from the error line,  $Y_i = \bar{T}X_i + b$ .

Since thermodynamic parameters for reactions are normally reported for the average temperature of determination and since  $\beta''$  equals  $\bar{T}$  or follows it closely, the second term in Eq. 9 will equal zero in most cases; the calculated values of  $\delta\Delta H'$  will equal  $\delta\Delta G$ . It is not surprising, therefore, that calculated  $\delta\Delta H'$  values are linear in  $\sigma$  for series that obey the Hammett relationship (Eq. 2) (4, 7, 8).

**Vertical and Horizontal Distances from Error Line**—While the Hepler model is satisfying from a mechanistic point of view, the method has two serious drawbacks. First,  $\bar{T}$  for the solvation effect is also equal to the error slope for any isergonic relationship. Second, the calculation of  $\delta\Delta H'$  from Eq. 8 is identical to the method used in calculating  $\delta\Delta G$  values for scatter about any isergonic line. Therefore, it is possible to obtain results identical to those of Hepler's without referring to a solvation mechanism merely by calculating the deviation in enthalpy or entropy from the error slope,  $\bar{T}$ .

The equations for an analysis based on distances from the error line may be formulated by reference to Fig. 1. The equation of the error line with a slope equal to  $\bar{T}$  and drawn through the coordinates of the parent point  $(Y_p, X_p)$  is given by:

$$Y_i = \bar{T}X_i + b \quad (\text{Eq. 10})$$

where  $b = \Delta H_{obs_p} - \bar{T}\Delta S_{obs_p}$  = free energy of parent compound, and  $Y_i$  and  $X_i$  represent  $\Delta H_{obs}$  and  $\Delta S_{obs}$  values for a given compound projected to the error line. The vertical distance of the observed point in the figure from the error line is given by the difference in  $\Delta H_{obs_i}$  and  $Y_1$  according to:

$$\Delta\Delta H_i = \Delta H_{obs_i} - \bar{T}\Delta S_{obs_i} - b \quad (\text{Eq. 11})$$

In a similar manner, the horizontal distance of the observed point from the error line is obtained as the difference between  $S_{obs_i}$  and  $X_2$ , which is equal to:

$$\Delta\Delta S_i = \Delta S_{obs_i} - (\Delta H_{obs_i}/\bar{T}) + b/\bar{T} \quad (\text{Eq. 12})$$

The corresponding free energy terms for the observed values calculated from the distances to the error line are obtained by substituting Eqs. 11 and 12 into the Gibbs free energy expression to obtain:

$$\Delta G_{obs_i} = \Delta\Delta H_i + b \quad (\text{Eq. 13})$$

and:

$$\Delta G_{obs_i} = -\bar{T}\Delta\Delta S_i + b \quad (\text{Eq. 14})$$

The values of  $\Delta\Delta H_i$  of Eq. 11 and  $\delta\Delta H'$  of Eq. 8 differ only by the constant  $b$ , which is equal to the free energy contribution of the parent compound. Furthermore, from Eqs. 13 and 14, it can be seen that the expression for  $\Delta G_{obs_i}$  is given as a sum of two free energy terms: one for the parent compound ( $b$ ) and one for the substituent ( $\Delta\Delta H_i$  or  $-\bar{T}\Delta\Delta S_i$ ). The vertical distance,  $\Delta\Delta H_i$ , or its counterpart on the horizontal axis,  $-\bar{T}\Delta\Delta S_i$ , simply yields the free energy contribution of the substituent symbolized by  $\delta\Delta G$ . Thus, series that obey the Hammett relationship (Eq. 2) will necessarily yield  $\Delta\Delta H_i$  values that correlate with  $\sigma$ .

**Lengths of Error Contours and Perpendicular Distances from**

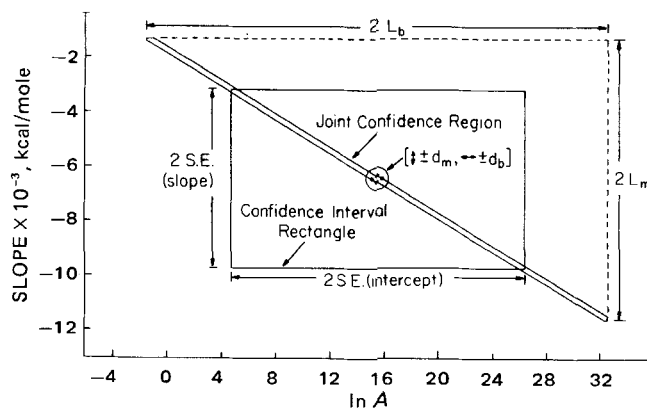


**Figure 2**—Comparison of the joint confidence region (error contour) and confidence interval rectangle associated with the slope and intercept of the Arrhenius fit for the alkaline hydrolysis of phenyl benzoate.

**$\beta$  Line**—The decision of whether to include any given member of a congeneric series within the classification of an assigned  $\beta$  value is arrived at by determining the error associated with that member on an isergonic profile. As stressed previously (1, 6), however, the uncertainty of any point on such a profile is not given by a rectangle with dimensions in standard errors for that point but instead by a region referred to as the error contour. The standard errors of  $\Delta H$  and  $\Delta S$  are appropriate when discussing either one of these two quantities independently of the other; but when both are considered jointly as in isergonic profiles, the correct uncertainty function is the joint confidence region (9). This region takes the shape of a highly eccentric ellipse when the variances of the two considered quantities differ widely and are strongly correlated. Such is the case for the least-squares estimates of the slope and intercept of Arrhenius plots from which  $\Delta H$  and  $\Delta S$  are derived.

Mandel and Linnig (10) pointed out that a negative correlation exists between the errors in slope and intercept whenever the  $x$  values of the original data are positive. As a consequence, the upper part of the error ellipse tilts toward the ordinate in a plot of slope versus intercept<sup>4</sup>. The boundaries of this ellipse are determined by the standard error of estimate,  $s$ , for the least-squares analysis and by the ( $F$  ratio)<sup>1/2</sup> for the desired confidence level. Thus, at any desired confidence level, only values of the slope and intercept that fall within the boundaries of the ellipse are allowed on the basis of observed experimental error.

Mandel and Linnig (10) simplified the plotting of joint confidence regions by deriving a function that closely approximates the error ellipse from three sets of parallel tangents. These parallel lines can be plotted on graph paper with the aid of four constants ( $L_m$ ,  $L_b$ ,  $d_m$ , and  $d_b$ ) describing the error function (see Appendix for equations). This method of ellipse construction was used to plot the joint error region associated with the slope and intercept of the Arrhenius fit for the alkaline hydrolyses of phenyl benzoates at 20, 30, and 35° (8). Figure 2 illustrates the extreme eccentricity of the error ellipse for this type of data as compared with the larger rectangular area based in the standard errors of the slope and intercept.

Two important features arise out of the error ellipse analysis as applied to the interpretation of isergonic profiles. First, the lengths of the error regions determine whether two or more points lying along an isergonic line are potentially interchanged as a result of experimental error. Second, the widths,  $w$ , or thicknesses of the error regions determine which points of an isergonic profile belong to a given interaction line with slope =  $\beta$ . Both of these features can be utilized by plotting all individual error contours on an isergonic profile and then observing their distribution relative to either the least-squares line drawn through the data or the error line with a slope of  $\bar{T}$ .

Since the process of plotting error contours on graph paper is tedious and time consuming, even for the Mandel-Linnig projections, an alternative method for providing the same information is desirable. A comparison of the contour lengths projected along a given  $\beta$  line is easily accomplished by computing the value of  $(\text{slope} \pm L_m)$  for each point and then visually inspecting the calculated limits for overlap between any

<sup>4</sup> A plot of  $\Delta H'$  versus  $\Delta S'$  for these data would yield an error ellipse with a positive slope because of the change in sign that occurs in converting the slope to  $\Delta H'$ .

**Table I—Activation Parameters for the Alkaline Hydrolysis of Substituted Phenyl Benzoates<sup>a</sup>**

Substituent ( $\sigma^-$ ) <sup>b</sup>	$\Delta G^\ddagger$ , kcal/mole	$\Delta H^\ddagger$ , kcal/mole	$\Delta S^\ddagger$ , cal/mole-deg
4-CH <sub>3</sub> (-0.17)	21.3	10.9	-34.8
H (0.00)	21.1	12.1	-29.7
4-F (0.062)	20.7	11.0	-32.4
4-Cl (0.226)	20.6	11.8	-29.3
3-CN (0.678)	19.9	10.3	-31.9
4-CN (1.00)	19.6	10.5	-30.2
4-NO <sub>2</sub> (1.27)	19.4	11.6	-25.8

<sup>a</sup> Activation parameters are based upon an initial linear least-squares fit of raw data (at 20, 30, and 35°) from Ref. 8 to the Arrhenius equation, where  $\Delta H^\ddagger = E_a - RT$ ,  $\Delta S^\ddagger = R [\ln kT - \ln (kT/h) + \Delta H^\ddagger/RT]$ ,  $\Delta G^\ddagger = \Delta H^\ddagger - T\Delta S^\ddagger$  (before rounding off), and  $T = (\Sigma T)/N = 301.3^\circ\text{K}$ . <sup>b</sup> Values of  $\sigma^-$ , the Hammett constant for substituted phenols, were taken from Table 2-17 of Ref. 13.

cluded in calculating the parameters given in Table I. The slopes and intercepts of the Arrhenius plots based on data at 20, 30, and 35° were significant at least at the 0.05 level, except the intercept for the parent compound which was significant at the 0.10 level.

Linear free energy and isergonic correlations for activation parameters of the phenyl benzoate series are given in Table II. Of the three parameters, only  $\Delta G^\ddagger$  is a linear function of  $\sigma^-$  (Eq. 16). Furthermore, Eq. 19 shows that the isergonic profile is highly scattered. From the Leffler-Grunwald analysis given previously, nonlinearity observed with Eqs. 17-19 could be viewed in terms of multiple contributions to the observed enthalpies (Eqs. 3 and 4). When more than one mechanism contributes to  $\Delta H$ ,  $\Delta S$ , or both, the separate contributions would not be expected to correlate with the same substituent parameter in either  $\Delta H$  or  $\Delta S$ , nor would a proportionality of effects be expected to exist between the mechanisms. Hence, the isergonic profile would be scattered.

**Vertical and Horizontal Distances from  $\beta$  Line**—The vertical ( $\Delta\Delta H^\ddagger$ ) and horizontal ( $\Delta\Delta S^\ddagger$ ) distances from the error slope ( $\beta = 301.3^\circ$ ) for the individual points on the isergonic profile (Table III) were calculated from the observed activation enthalpies and entropies before rounding off, using Eqs. 11 and 12, respectively. The vertical distance of each substituent from the error line is identical to its substituent effect,  $\delta\Delta G^\ddagger$ , in agreement with Eq. 13. Similarly, on the horizontal scale,  $\delta\Delta G^\ddagger$  may be obtained as the product of  $\Delta\Delta S^\ddagger$  times  $-\bar{T}$ , which is in agreement with Eq. 14.

Linear free energy correlations for the vertical and horizontal distances are presented in Table IV. For  $\beta = 301.3^\circ$ , the resulting  $F$  ratios and correlation coefficients,  $r$ , are identical to those of Eq. 16 in Table II, demonstrating the redundancy between  $\Delta G^\ddagger$ ,  $\Delta\Delta H^\ddagger$ , and  $\Delta\Delta S^\ddagger$  as parameters for correlation with  $\sigma^-$ . Correlations based on  $\Delta\Delta H^\ddagger$  and  $\Delta\Delta S^\ddagger$  simply do not add any new information to the previously determined substituent effect based on  $\Delta G^\ddagger$  (Eq. 16).

Table IV also gives correlations for  $\Delta\Delta H^\ddagger$  versus  $\sigma^-$  when  $\beta$  is varied using the values of  $\Delta H^\ddagger$  and  $\Delta S^\ddagger$  at 301.3°. The analysis demonstrates the effect upon  $F$  and  $r$  when  $\beta$  equals some value other than the error slope,  $\bar{T}$ . When  $\beta$  varies between 0 and 600°K, the correlation coefficient takes on values between -0.215 and -0.910, with a maximum appearing at  $\beta = 325^\circ$ . For  $\beta = 0^\circ$ , the resulting  $\Delta\Delta H^\ddagger$  values equal  $\delta\Delta H^\ddagger$ ; the resulting  $F$  and  $r$  values for the correlation are identical to those for Eq. 17 (Table II) based on  $\Delta H^\ddagger$ .

Values of  $\beta$  between 280 and 325° closely approximate the limits of  $\beta$

**Table II—Correlations for Activation Parameters<sup>a</sup>**

Regression Equations <sup>b</sup> ( $n = 7$ )	S	F	r	Equation Number
$\Delta G^\ddagger = -1.33\sigma + 21.0$	0.136	175	-0.986	16
$\Delta H^\ddagger = -0.268\sigma + 11.3$	0.733	0	-0.215	17
$\Delta S^\ddagger = 3.53\sigma - 32.1$	2.27	4	-0.684	18
$\Delta H^\ddagger = 134\Delta S^\ddagger + 15,300$	625.0	2	-0.554	19

<sup>a</sup>  $n$  = number of data points used in linear least-squares fit;  $S$  = standard error of estimate;  $r$  = correlation coefficient; and  $F = F$  ratio (at the 90 and 95% confidence levels,  $F = 4.06$  and  $6.61$ , respectively, for 1,5 degrees of freedom). <sup>b</sup> Equations 16 and 17 are expressed in kcal/mole, Eq. 18 is expressed in cal/mole-deg, and Eq. 19 is expressed in cal/mole.

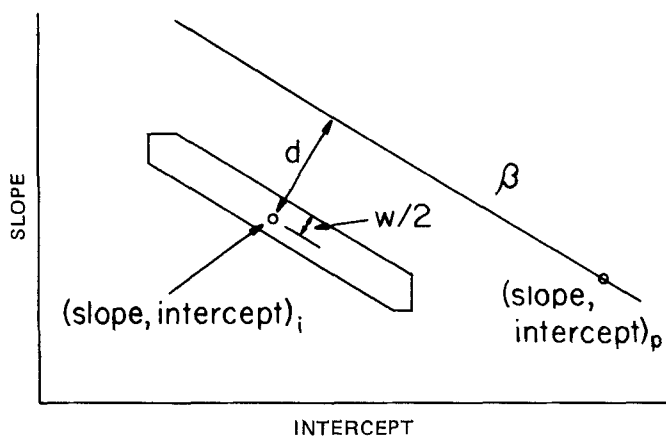


**Figure 3**—Diagram showing the perpendicular distances  $d$  (distance from center of error ellipse to  $\beta$  line drawn through parent point) and  $w/2$  (distance from center to ellipse boundary).

points. These limits should not overlap if one wishes to gain statistical confidence in the relative positioning of points along the line.

The use of contour widths to interpret isergonic data requires a comparison between the perpendicular half-widths,  $w/2$ , of the contours and the respective perpendicular distances,  $d$ , from a given  $\beta$  line (Fig. 3). These distances may be calculated from Eq. 15 which, in general, gives the perpendicular distance,  $p$ , of any point from a given line (11):

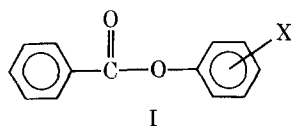
$$p = (AX_i + BY_i + C)/(A^2 + B^2)^{1/2} \quad (\text{Eq. 15})$$

where  $X_i$  and  $Y_i$  are the coordinates of the point and where the equation for the line is given by  $AX + BY + C = 0$ , with  $X$  and  $Y$  representing the coordinates for a point on the line. The coefficients  $A$ ,  $B$ , and  $C$  may be expressed in terms of the more usual slope-intercept form for a line,  $Y = mX + b$ , as follows:  $A = -m$ ,  $B = 1$ , and  $C = -b = -(Y - mX)$ . For calculating the distance,  $d$ , in Fig. 3 from the line drawn through the parent point, these coefficients take on the values  $A = -\beta$ ,  $B = 1$ , and  $C = -[\text{slope}_p - \beta(\text{intercept}_p)]$ . For calculating the distance,  $w/2$ , in the figure from the contour limit extending through a point with coordinates of  $(\text{slope}_i + dm; \text{intercept}_i)$ , the coefficients take on the values  $A = -L_m/L_b$ ,  $B = 1$ , and  $C = -[(\text{slope}_i + dm) - L_m/L_b(\text{intercept}_i)]$ .<sup>5</sup> A comparison between the values of  $d$  and  $w/2$  for each point indicates whether the point belongs to the particular  $\beta$  line in question. Thus, a point may be rejected at the confidence level of its error contour when  $d > w/2$ .

## RESULTS AND DISCUSSION

The data chosen for analysis are those of Washkuhn *et al.* (8) for the alkaline hydrolysis of 3- or 4-substituted phenyl benzoates (I), where  $X = 4\text{-CH}_3$ ,  $\text{H}$ ,  $4\text{-F}$ ,  $4\text{-Cl}$ ,  $3\text{-CN}$ ,  $4\text{-CN}$ , or  $4\text{-NO}_2$ . This congeneric series obeys the Hammett relationship (Eq. 2) but shows a scattered  $\Delta H$  versus  $\Delta S$  profile. Therefore, it is suitable for analysis using the equations given previously. The second-order rate constants,  $k_{\text{OH}}$ , for the series were reported as a function of temperature at 20, 25, 30, and 35° determined in 50% (v/v) acetonitrile-0.02  $M$  phosphate buffer.

**Activation Parameters**—A preliminary graphical plot of the data showed a large systemic deviation of the rate constant at 25° for each member of the series. These displaced data points were tested for exclusion from further data analysis by determining the significance probability of the  $t$  value under such conditions (12). In all cases, the significance levels were considerably greater than 0.05, justifying a rejection of the null hypothesis. From these results and because of the large upward systemic displacement of each point, data at 25° were not in-



<sup>5</sup> From the Appendix,  $L_m/L_b = (N/\Sigma X^2)^{1/2} = [N/\Sigma (1/T)^2]^{1/2}$  while  $\bar{T} = (\Sigma T)/N$ . The difference between these two quantities, however, is small ( $\approx 0.3^\circ\text{K}$ ) for the usual 20° temperature range used in collecting Arrhenius data.

**Table III—Comparison between Substituent Effects ( $\delta\Delta G^\ddagger$ ) and Vertical ( $\Delta\Delta H^\ddagger$ ) and Horizontal ( $\Delta\Delta S^\ddagger$ ) Distances from the Error Slope,  $\beta = 301.3^\circ$**

Substituent	$\delta\Delta G^\ddagger$ , cal/mole	$\Delta\Delta H^\ddagger$ , cal/mole	$\Delta\Delta S^\ddagger$ , cal/mole-deg
4-CH <sub>3</sub>	269	269	-0.894
H (none)	0	0	0
4-F	-324	-324	1.074
4-Cl	-483	-483	1.602
3-CN	-1143	-1143	3.792
4-CN	-1450	-1450	4.813
4-NO <sub>2</sub>	-1669	-1669	5.538

<sup>a</sup>  $\delta\Delta G = \Delta C_{X^\ddagger} - \Delta C_{H^\ddagger}$ ;  $\Delta\Delta H^\ddagger$  and  $\Delta\Delta S^\ddagger$  were calculated using Eqs. 11 and 12, respectively.

for aqueous solvation effects in phenols as suggested by Hepler (270° <  $\beta$  < 320°) (4). Within this range of  $\beta$ , the value of  $r$  for the  $\Delta\Delta H^\ddagger$  versus  $\sigma^-$  correlations is observed to change only very slightly, and deviations in the slopes from  $\bar{T}$  are not statistically significant even at the 50% level. Alternatively, it may be stated that values of  $\beta$  between 280 and 325°K for a proposed solvation mechanism could not be distinguished statistically from  $\bar{T}$  falling within this temperature region.

**Lengths of Error Contours**—The constants  $L_m$ ,  $L_b$ ,  $d_m$ , and  $d_b$  were calculated for each member of the series, using the method of Mandel and Linnig (10) outlined in the Appendix. Based upon the values of  $L_m$  and the slope values for Arrhenius fits to the data, limits for lengths of error contours are given in Table V for the 90% confidence level. A visual inspection of these limits shows that each member of the series is overlapped to some extent by every other member of the series. If the individual data points for the present series fell upon a single isergonic line,  $\beta = \bar{T}$ , the result could only be attributed to experimental error.

The extreme overlap of error contours for this series is a function of: (a) the small number of data points,  $N$ , available for the Arrhenius fits; (b) the experimental error as reflected by  $S^2$  (error variance); and (c) the narrow range of slope values (0.9 kcal/mole), which produces small differences between the individual members. The first two factors are included in the constant,  $K$  (Eq. A5), which determines the length of the error contour. If  $S^2$  is maintained at the same level, simply increasing  $N$  for the Arrhenius fits would considerably reduce the lengths of the contours. Thus, lengths would be decreased by a factor of  $[(F_{df} = 1)/(F_{df} = x)]^{1/2}$  for each additional increase in  $N$  above  $N = 3$ . For  $N = 4$  and  $N = 5$ , the contour lengths decrease by factors of 2.35 and 3.01, respectively, at the 90% confidence level. For the present series, however, these decreases in contour lengths are not sufficient to eliminate their overlap because of the small differences between the slopes. Extremely precise data yielding very small values of  $S^2$  would be required to remove the overlap.

**Perpendicular Distances from  $\beta$  Line**—As discussed under *Theoretical*, perpendicular distances represented by  $d$  and  $w/2$  may be utilized to determine whether the individual members of a series belong to a given  $\beta$  line. These values for the present series are given in Table VI for vari-

**Table V—Limits for Lengths of Error Contours at 90% Confidence Level<sup>a</sup>**

Substituent	Slope + $L_m$ , kcal/mole	Slope - $L_m$ , kcal/mole
4-CH <sub>3</sub>	-4.64	-6.89
H (none)	-1.26	-11.6
4-F	-3.22	-8.44
4-Cl	-2.35	-10.1
3-CN	-3.23	-7.74
4-CN	-2.57	-8.60
4-NO <sub>2</sub>	-4.55	-7.76

<sup>a</sup> Slope =  $-(E_d/R)$ , obtained from a linear least-squares fit of the data (at 20, 30, and 35°) to the Arrhenius equation. The  $L_m$  values were calculated from Eq. A1 (see Appendix). The  $F$  ratio = 49.5 for 2,1 degrees of freedom at the 0.90 level.

ations in  $\beta$  and in significance levels. The perpendicular distances for the members of the series from the error line ( $d_{301.3}$ ) is greater than their respective contour widths ( $w/2$ ) measured perpendicularly to the contour boundary (Table VI). This comparison is good at both the 90 and 95% confidence levels. A similar comparison between  $d$  values measured from  $\beta = 280^\circ$  and  $325^\circ$  and their respective  $w/2$  values produces the same results.

From the comparisons based on a  $\beta$  line of 301.3°, it is certain that the points do not fall along the error line or that the distribution of points on the isergonic profile is strongly affected by the correlation of error producing this line. The influence of a heavily weighted error slope would force the distribution of points along a slope of  $\beta = \bar{T}$ . This is not the case here since, from the previous  $\Delta H^\ddagger$  versus  $\Delta S^\ddagger$  correlation (Eq. 19),  $\beta = 134^\circ$  and  $r = -0.554$ . Pure error would produce a perfect correlation between  $\Delta H^\ddagger$  and  $\Delta S^\ddagger$ , with the resultant slope being equal to  $\bar{T}$ .

The  $\Delta d$  values given in Table VI provide a means of determining whether  $\beta = 301.3^\circ$  is different from either  $\beta = 280^\circ$  or  $\beta = 325^\circ$ , the latter being close to the suggested limits for solvation effects in phenols (4). A comparison of either  $\Delta^1$  or  $\Delta^2$  (differences in  $d$  from either side of the error line) with the respective  $w/2$  values for the 95% confidence level shows that the differences,  $\Delta d$ , fall within the error range of the perpendicular contour widths,  $w/2$ . The comparisons are approximately as good at the 90% confidence level. These results indicate that  $\beta = 301.3^\circ$  cannot be distinguished from  $\beta = 280$  or  $325^\circ$ .

The  $d$  values for each substituent at a given value of  $\beta$  follow a trend resembling its substituent effect (Table VI). Correlations between  $d$  and  $\sigma^-$  for values of  $\beta$  ranging between 0 and 600° are given in Table IV. The values of  $F$  and  $r$  obtained over the range of  $\beta$  for these correlations are identical to those values obtained for the correlation between  $\Delta\Delta H^\ddagger$  and  $\sigma^-$  (Table IV). While a comparison between values of  $d$  and  $w/2$  aids in the classification of  $\beta$  values, the absolute values of  $d$  identically parallel substituent effects ( $\delta\Delta G^\ddagger$ ) and, therefore, provide no new information about substituent effects for the series.

## CONCLUSIONS

The present analysis shows that the geometric distances of data points on an isergic profile, calculated either in the vertical ( $\Delta\Delta H$ ), horizontal ( $\Delta\Delta S$ ), or perpendicular ( $d$ ) distances from the error slope, do not add any new information to a substituent effect analysis already based on  $\Delta G$ . The vertical distances,  $\Delta\Delta H$ , are identical to the substituent effect  $\delta\Delta G$ ; for series that obey the Hammett relationship (Eq. 2), these distances must correlate with  $\sigma^-$  regardless of the implication of a solvation mechanism. Thus, the use of the Hepler method (Eq. 8) to demonstrate a solvation effect in the scattered isergonic profile for series I would not be warranted. This conclusion does not deny the existence of a solvation mechanism for the series but does seriously question the Hepler approach for implicating the mechanism.

Statistically, the use of the joint confidence region (error contour) is the soundest way of analyzing the distribution of points on an isergonic profile. The method is simple and should routinely accompany such profiles appearing in the literature. The limits of the error contour lengths provide evidence of overlap between members of the series and, hence, dictate statistical uncertainty along the line. For series such as I, which do not show a wide variation in substituent effects, extremely precise rate data with  $N = 4$  or  $5$  would be required to eliminate overlap between contours.

Leffler (6) suggested testing the randomness of the data along the isergonic line when overlap cannot be eliminated. Thus, points appearing

**Table IV—Correlations for Distances from the  $\beta$ -Line**

$\beta$	Slope	Intercept	$F$	$r$
Vertical Distances <sup>a</sup> ( $\Delta\Delta H^\ddagger$ versus $\sigma^-$ )				
0	-268	-839	0	-0.215
280	-1260	-153	118	-0.979
301.3	-1330	-102	175	-0.986
325	-1420	-43.6	211	-0.988
600	-2390	630.0	24	-0.910
Horizontal Distances <sup>a</sup> ( $\Delta\Delta S^\ddagger$ versus $\sigma^-$ )				
301.3	4.42	0.337	175	0.986
Perpendicular Distances ( $d$ versus $\sigma^-$ )				
0	135	422	0	-0.215
280	2.26	0.276	118	0.979
301.3	2.23	0.170	175	0.986
325	2.19	0.0674	211	0.988
600	2.00	0.528	24	0.910

<sup>a</sup> The intercepts for vertical and horizontal distances are expressed in calories per mole and calories per mole-degree, respectively.

Table VI—Comparison between  $d$  and  $w/2$  Values<sup>a</sup>

Substituent	$d$ Values			$\Delta d^b$		$w/2$ Values <sup>c</sup>	
	$\beta = 280$	$\beta = 301.3$	$\beta = 325$	$\Delta^1$	$\Delta^2$	$CL = 0.90$	$CL = 0.95$
4-CH <sub>3</sub>	-0.290	-0.450	-0.604	0.154	0.160	0.078	0.157
H (none)	0	0	0	0	0	0.357	0.717
4-F	0.685	0.540	0.402	0.138	0.145	0.181	0.363
4-Cl	0.852	0.806	0.763	0.043	0.046	0.269	0.540
3-CN	2.140	1.908	1.686	0.222	0.232	0.156	0.314
4-CN	2.628	2.421	2.224	0.197	0.207	0.209	0.419
4-NO <sub>2</sub>	2.849	2.787	2.727	0.060	0.062	0.111	0.223

<sup>a</sup> The  $d$  and  $w/2$  values were calculated using Eq. 15 and the values of the coefficients  $A$ ,  $B$ , and  $C$  described in the text. <sup>b</sup>  $\Delta^1$  and  $\Delta^2$  refer to the differences ( $d_{301.3} - d_{325}$ ) and ( $d_{280} - d_{301.3}$ ), respectively. <sup>c</sup>  $CL$  = confidence level.

along the line in an order that also follows their  $\sigma$  values could still represent a real effect. A comparison between the  $d$  and  $w/2$  values provides a means of determining whether the points falling along an isergonic line differ statistically from those falling along another line such as the error line. For series such as I with scattered isergonic profiles, a result of  $d > w/2$  simply proves that the scatter is not the result of experimental error.

A further comparison between differences in  $d$ ,  $\Delta d$ , from various  $\beta$  lines and  $w/2$  values provides a means of establishing a  $\beta$  range for the error contour. When using suggested  $\beta$  lines for solvation effects, this range for series I was approximately 45°. Since the average reaction temperature,  $\bar{T}$ , fell within this range, it must be concluded that solvation effects could not be distinguished statistically from error effects.

#### APPENDIX

Equations A1–A4 give the relationships for computing the four constants ( $L_m$ ,  $L_b$ ,  $d_m$ , and  $d_b$ ) required in constructing the joint confidence region from three sets of parallel tangents (10):

$$L_m = K(N/\Delta)^{1/2} \quad (\text{Eq. A1})$$

$$L_b = K(Q/\Delta)^{1/2} \quad (\text{Eq. A2})$$

$$d_m = K[2W/Q(1 + W)]^{1/2} \quad (\text{Eq. A3})$$

$$d_b = d_m(L_b/L_m) \quad (\text{Eq. A4})$$

Definitions of the symbols appearing in these equations are further given by Eqs. A5–A8:

$$K = (2FS^2)^{1/2} \quad (\text{Eq. A5})$$

$$\Delta = N\sum X^2 - (\sum X)^2 \quad (\text{Eq. A6})$$

$$Q = \sum X^2 \quad (\text{Eq. A7})$$

$$W = (N\sum X^2)^{1/2}/\sum X \quad (\text{Eq. A8})$$

where  $F$  =  $F$  ratio for 2 and  $N - 2$  degrees of freedom at the desired confidence level,  $S^2$  = the error variance for the least-squares analysis,

$N$  = total number of data pairs, and  $X$  =  $X$  value for data pair.

The joint confidence region is constructed within a rectangle having the dimensions of  $2L_m$  for the ordinate and  $2L_b$  for the abscissa, as observed in Fig. 2. A diagonal line with a negative slope running from corner to corner through the rectangle forms the major axis of the simulated ellipse, thus producing a tilt slope of  $L_m/L_b$ . Plotted values  $\pm d_m$  in the ordinate direction and  $\pm d_b$  in the abscissa direction from the center of the rectangle form the guide points for drawing the two sloping major ellipse boundaries (Fig. 2).

#### REFERENCES

- (1) J. E. Leffler and E. Grunwald, "Rates and Equilibrium of Organic Reactions," Wiley, New York, N.Y., 1963, chap. 9.
- (2) R. L. Schowen, *J. Pharm. Sci.*, **56**, 931 (1967).
- (3) R. Lumry and S. Rajender, *Biopolymers*, **9**, 1125 (1970).
- (4) L. G. Hepler, *J. Am. Chem. Soc.*, **85**, 3089 (1963).
- (5) L. G. Hepler, *Can. J. Chem.*, **49**, 2803 (1971).
- (6) J. E. Leffler, *J. Org. Chem.*, **31**, 533 (1966).
- (7) J. Zimmerman and S. J. Yau, *J. Pharm. Sci.*, **62**, 902 (1973).
- (8) R. J. Washkuhn, V. I. Patel, and J. R. Robinson, *ibid.*, **60**, 736 (1971).
- (9) N. R. Draper and H. Smith, "Applied Regression Analysis," Wiley, New York, N.Y., 1966, chap. 2.
- (10) J. Mandel and F. J. Linnig, *Anal. Chem.*, **29**, 743 (1957).
- (11) W. L. Hart, "Elements of Analytic Geometry," D. C. Heath, Boston, Mass., 1950, chap. 2.
- (12) G. W. Snedecor and W. G. Cochran, "Statistical Methods," 6th ed., Iowa State University Press, Ames, Iowa, 1967, chap. 6.
- (13) K. B. Wiberg, "Physical Organic Chemistry," Wiley, New York, N.Y., 1964, Part 2-8.

#### ACKNOWLEDGMENTS AND ADDRESSES

Received November 21, 1975, from the Department of Pharmaceutics, School of Pharmacy, Temple University, Philadelphia, PA 19140.  
Accepted for publication March 1, 1976.